

Design, Synthesis, and SAR Study of a Series of *N*-Alkyl-*N'*-[2-(aryloxy)-5-nitrobenzenesulfonyl]ureas and -cyanoguanidine as Selective Antagonists of the TP α and TP β Isoforms of the Human Thromboxane A₂ Receptor

Julien Hanson,^{*,†} Jean-Michel Dogné,^{†,§} Jérémie Ghiotto,[†] Anne-Lise Moray,[†] B. Therese Kinsella,[‡] and Bernard Pirotte[†]

Drug Research Center, Laboratory of Medicinal Chemistry, University of Liège, 1, Av. de l'Hôpital, B-4000 Liège, Belgium, School of Biomolecular & Biomedical Science, Conway Institute for Biomolecular and Biomedical Research, University College Dublin, Ireland, and Department of Pharmacy, University of Namur, FUNDP, 61 rue de Bruxelles, B-5000 Namur, Belgium

Received April 11, 2007

The prostanoid thromboxane (TX)A₂ exerts its proaggregant and constrictive actions upon binding to the specific TXA₂ receptor (TP), a member of the G-protein coupled receptor superfamily. In humans, TXA₂ signals through two distinct TP isoforms, TP α and TP β . Herein, we describe the design, synthesis, and SAR study of a series of original *N*-alkyl-*N'*-[2-(aryloxy)-5-nitrobenzenesulfonyl]ureas and -cyanoguanidine. The SAR study was based on the results of a functional assay, TP-mediated intracellular calcium ([Ca²⁺]_i) mobilization performed on the two separate isoforms. Optimal nature and position of several structural moieties was defined for both activity and selectivity toward TP α and TP β isoforms. Three compounds (**9h**, **9af**, and **9ag**), showing increased selectivity for TP β relative to TP α (23.2:1, 18.1:1, 19.9:1, respectively), were selected for further experiments, and their activity was confirmed in a platelet aggregation assay. This study represents the first extended SAR study dealing with the identification of isoform selective antagonists for the human TXA₂ receptor.

Introduction

The lipid mediator thromboxane (TX)A₂ plays a key role in several physiologic processes including platelet aggregation and vascular and bronchial smooth muscle constriction.^{1,2} An overproduction of TXA₂^a has been associated with many pathological states such as myocardial infarction, thrombosis, unstable angina, pulmonary embolism, septic shock, atherosclerosis, preeclampsia, and asthma.³ TXA₂, a metabolite of arachidonic acid (AA) released mainly by phospholipase (PL)-A₂ from membrane phospholipids, is primarily synthesized through the sequential actions of cyclooxygenase (COX) and TX synthase in platelets.³

The actions of TXA₂ are mediated by its specific G-protein coupled receptor (GPCR), referred to as the TXA₂ receptor or TP.⁴ In 1991, Hirata et al. reported that the human TP is encoded by one gene,⁵ and in 1994 Raychowdhury et al. identified the existence of a second isoform generated by alternative splicing.⁶ The two human TP isoforms, namely TP α and TP β , share the first 328 amino acids but differ within their carboxyl-terminal tails (the last 15 amino acids of the α isoform being replaced by 79 amino acids in the β isoform). To date, the exact role of the TP α and TP β isoforms is not fully understood although several studies have established that they may have distinct physiological functions.^{7–9} It has been proposed, for example, that specific antagonism of TP β would be useful to enhance revascularization postmyocardial infarction since the stimulation of TP β seemed to be responsible for vascular endothelial growth factor-induced endothelial cell differentiation and migration.¹⁰

On the other hand, because TP α appears to be the predominant TP isoform expressed in platelets,¹¹ specific inhibitor(s) of TP α may be beneficial as more specific antiplatelet agent(s).

Hence, the design and synthesis of selective isoform specific TP receptor antagonists would be of great interest not only in therapeutics but also as tools in pharmacological sciences to decipher TP isoform specific roles. Despite great interest, the identification of such TP α and/or TP β isoform specific agonists/antagonists has been poorly studied. Although early pharmacological reports have described selective TXA₂ receptor (TP) antagonists for separate tissues, the initial observations have never been confirmed on isolated TP isoforms.¹² Through previous investigations, our group has addressed the influence of the chemical structure of a series of nitrobenzenesulfonylureas and -cyanoguanidines on selective antagonistic potency for TP α or TP β .¹³ In that study, we reported the synthesis and functional characterization of a series of derivatives of the potent TP receptor antagonist **1** (BM573, Figure 1),¹⁴ and from such investigations a family of original *N*-alkyl-*N'*-[2-(4-methylphenoxy)-5-nitrobenzenesulfonyl]urea compounds was selected for further detailed characterization through both chemical optimization and functional biologic/pharmacologic readouts. Three of the most interesting previously reported compounds **2**, **3**, and **4** are illustrated in Figure 1. In the present study, we describe the design, synthesis, and SAR study of a series of original nitrobenzenesulfonylureas derived from the latter **2**, **3**, and **4** chemical leads. We have characterized the antagonistic potency and TP-isoform selectivity of the new compounds using a functional pharmacological test, namely inhibition of intracellular calcium ([Ca²⁺]_i) mobilization in model mammalian cell lines that specifically overexpress the individual TP α or TP β isoforms. The antiplatelet activity of some of the most interesting compounds was also determined in aggregation assays.

Chemistry. The compounds evaluated in this work were synthesized according to the synthesis pathway described in Schemes 1–3. In the first step, which is common to all

* To whom correspondence should be addressed. Phone: +3243664382, fax: +3243664362, e-mail: J.hanson@ulg.ac.be.

[†] University of Liège.

[‡] University College Dublin.

[§] University of Namur.

^a Abbreviations: TXA₂, thromboxane A₂; TXS, thromboxane synthase; PLA₂, phospholipase A₂; AA, arachidonic acid; GPCR, G-protein coupled receptor; COX, cyclooxygenase; TP, thromboxane receptor; PLC, phospholipase C; IP₃, inositol 1,4,5-triphosphate.

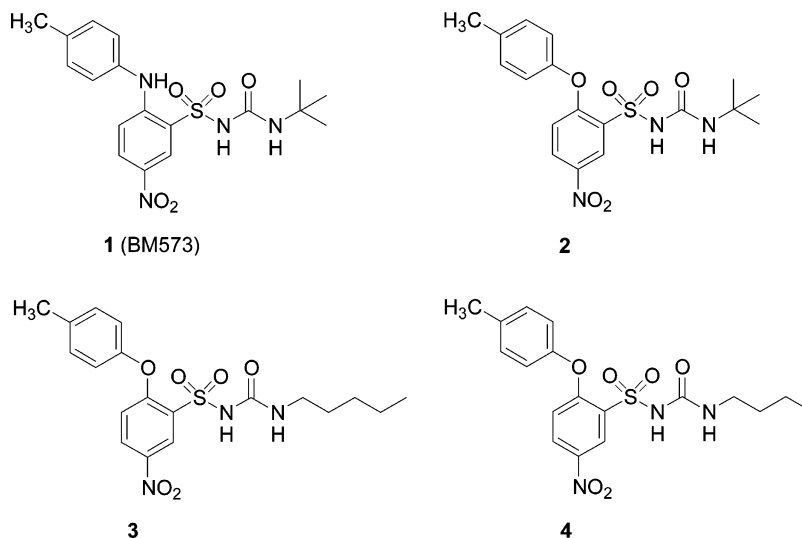
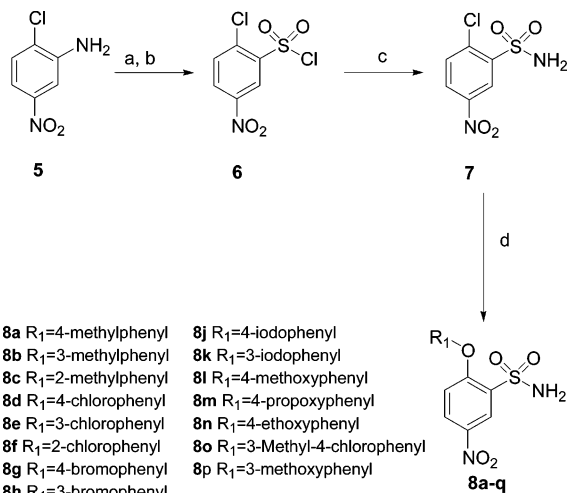


Figure 1. Chemical structures of 1–4.

Scheme 1^a



^a Reagents: (a) NaNO₂, HCl; (b) SO₂, HOAc, Cu₂Cl₂; (c) NH₄OH, Δ; (d) appropriate phenolate, acetonitrile, K₂CO₃.

compounds described, commercially available 2-chloro-5-nitroaniline (**5**) reacted with sodium nitrite in acidic medium, and the resulting diazonium salt solution was mixed with a solution of sulfur dioxide in acetic acid in the presence of Cu(I) to generate 2-chloro-5-nitrobenzenesulfonyl chloride (**6**) according to the Meerwein variation of the Sandmeyer reaction.¹⁵ Compound **6** was poured into a solution of ammonium hydroxide and gently heated, resulting in the synthesis of 2-chloro-5-nitrobenzenesulfonamide (**7**) which is the common intermediate giving access to the compounds studied (Scheme 1).

The nucleophilic substitution of the chlorine atom in the para position to the nitro group by various phenols led to the synthesis of the intermediates **8a–p**. Deprotonation of the sulfonamide group of compounds **8a–p** followed by reaction with the appropriate isocyanate led to the synthesis of compounds **9a–aj** (Scheme 2).

For the synthesis of the sulfonylcyanoguanidine **12**, a reactive synthon was first prepared by direct reaction of diphenyl *N*-cyanoiminocarbonate (**10**) with *tert*-butylamine. This synthon (**11**) directly reacted with the sulfonamidate salt of **8a** (**9**) to generate compound **12** (Scheme 3).

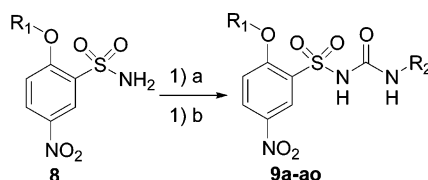
Pharmacological Evaluation. Thereafter, we wished to address the structure–activity relationships (SAR) of the latter

compounds based on a functional pharmacological evaluation. To this end, the ability of the compounds to antagonize TPα- and TPβ-mediated intracellular calcium ([Ca²⁺]_i) mobilization in response to the TXA₂ mimetic U46619 (5-heptenoic acid, 7-[(1*R*,4*S*,5*S*,6*R*)-6-[(1*E*,3*S*)-3-hydroxy-1-octenyl]-2-oxabicyclo-[2.2.1]hept-5-yl]-, (5*i*)-(9*CI*)) was evaluated in human embryonic kidney (HEK) 293 cell lines stably overexpressing either TPα (HEK·TPα cells) or TPβ (HEK·TPβ cells). Indeed, both TPα and TPβ are coupled to the Gq/phospholipase C effector system⁸ and, hence, can readily induce a rise in [Ca²⁺]_i upon agonist stimulation of the TP receptor. HEK·TPα and/or HEK·TPβ cells were preloaded with Ca²⁺ fluorescent dye Fluo-4, and inhibition of [Ca²⁺]_i mobilization in response to the well characterized TXA₂ mimetic U46619 (1 μM) stimulation was determined in the absence or presence of increasing concentrations of the test compounds, using concentrations ranging from 10⁻⁹ M to 10⁻⁵ M. Concentration–response curves were determined, and the IC₅₀, defined as the concentration (*M*) of compound required to inhibit 50% of U46619-induced [Ca²⁺]_i mobilization, values of *M* were calculated for each compound tested. A selectivity index, defined as ratio of the IC₅₀ (*M*) of TPα relative to the IC₅₀ (*M*) of TPβ (i.e., IC₅₀ TPα/IC₅₀ TPβ) was subsequently determined.

Furthermore, since TXA₂ is a potent inducer of platelet aggregation, the ability of the most interesting test compounds to prevent aggregation of human platelets in response to the TXA₂ mimetic U46619 was also evaluated. In this test, the compounds were incubated at concentrations ranging from 10⁻⁹ to 10⁻⁵ M with isolated human platelets, and aggregation was triggered upon stimulation by U46619 (1 μM).

Results and Discussion

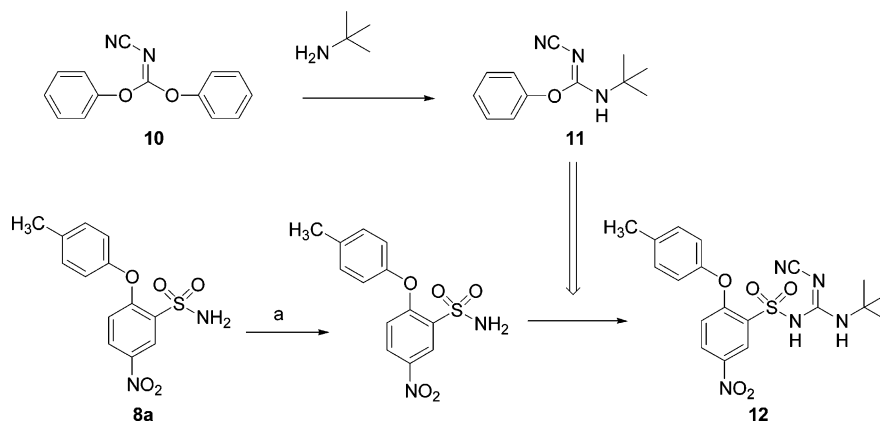
In a previous study, we demonstrated the activity of a family of nitrobenzenesulfonylureas presenting an oxygen bond between the two aromatic rings as selective antagonists of the TPα and TPβ isoforms of the human TXA₂ receptor (TP).¹³ The three most interesting leads identified in those previous investigations,¹³ namely compounds 2–4, are presented in Figure 1 and their relative potency toward the TP receptor isoforms in Table 1. One single parameter was modulated in that preliminary study, namely the side chain on the sulfonylurea group. Consequently, herein, we designed and synthesized several series of *N*-alkyl-*N'*-[2-(aryloxy)-5-nitrobenzenesulfonyl]ureas, derived from 2–4 (Figure 1) in order to more precisely estimate the

Scheme 2^a

9a R₁ = 3-methylphenyl, R₂ = *n*-pentyl
9b R₁ = 2-methylphenyl, R₂ = *n*-pentyl
9c R₁ = 2-methylphenyl, R₂ = *i*-propyl
9d R₁ = 2-methylphenyl, R₂ = *n*-butyl
9e R₁ = 2-methylphenyl, R₂ = *t*-butyl
9f R₁ = 3-methylphenyl, R₂ = *i*-propyl
9g R₁ = 3-methylphenyl, R₂ = *n*-butyl
9h R₁ = 3-methylphenyl, R₂ = *t*-butyl
9i R₁ = 4-methylphenyl, R₂ = *i*-propyl
9j R₁ = 4-methylphenyl, R₂ = *n*-propyl
9k R₁ = 2-bromophenyl, R₂ = *t*-butyl
9l R₁ = 2-bromophenyl, R₂ = *n*-pentyl
9m R₁ = 3-bromophenyl, R₂ = *t*-butyl
9n R₁ = 3-bromophenyl, R₂ = *n*-pentyl
9o R₁ = 4-bromophenyl, R₂ = *t*-butyl
9p R₁ = 4-bromophenyl, R₂ = *n*-pentyl
9q R₁ = 2-chlorophenyl, R₂ = *t*-butylamino
9r R₁ = 2-chlorophenyl, R₂ = *n*-pentyl

9s R₁ = 3-chlorophenyl, R₂ = *t*-butyl
9t R₁ = 3-chlorophenyl, R₂ = *n*-pentyl
9u R₁ = 4-chlorophenyl, R₂ = *t*-butyl
9v R₁ = 4-chlorophenyl, R₂ = *n*-pentyl
9w R₁ = 3-iodophenyl, R₂ = *t*-butyl
9x R₁ = 3-iodophenyl, R₂ = *n*-pentyl
9y R₁ = 4-iodophenyl, R₂ = *t*-butyl
9z R₁ = 4-iodophenyl, R₂ = *n*-pentyl
9aa R₁ = 4-methoxyphenyl, R₂ = *t*-butyl
9ab R₁ = 4-methoxyphenyl, R₂ = *n*-pentyl
9ac R₁ = 4-propoxyphenyl, R₂ = *t*-butyl
9ad R₁ = 4-propoxyphenyl, R₂ = *n*-pentyl
9ae R₁ = 4-ethoxyphenyl, R₂ = *t*-butyl
9af R₁ = 4-ethoxyphenyl, R₂ = *n*-pentyl
9ag R₁ = 3-methoxyphenyl, R₂ = *t*-butyl
9ah R₁ = 3-methyl-4-chlorophenyl, R₂ = *t*-butyl
9ai R₁ = 3-methyl-4-chlorophenyl, R₂ = *n*-pentyl
9aj R₁ = 2-methoxy-4-methylphenyl, R₂ = *n*-pentyl

^a Reagents: (a) NaOH 10%; (b) R₂-N=C=O.

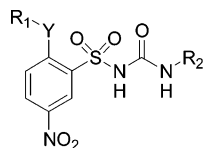
Scheme 3^a

^a Reagents: (a) NaOH 10%.

structure–activity relationships (SAR) for activity and selectivity within this family of compounds toward the individual TP receptor isoforms.

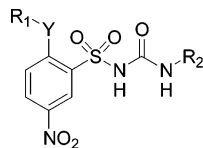
Several features of the structure were explored. Previous work on nitrobenzene sulfonyleurea suggested that the position and the nature of the nitro group as well as the position of the sulfonyleurea moiety and the second aromatic ring were optimal, so these parameters were kept constant (Dogné et al., unpublished data). As shown in Table 1, we first varied the position of the methyl group on the aromatic ring R₁ (2- and 3-position), and we addressed the influence of various alkyl side chains R₂ for each position. We also completed the series of side chains in the R₁ = 4-methylphenyl moiety series. All compounds examined in the U46619-mediated [Ca²⁺]_i mobilization assay displayed potent micro- and submicromolar IC₅₀ activities. Consistent with previous observations, all compounds tested were more potent on TPβ than on TPα¹³ in this assay. Throughout the studies presented in Tables 1–4, **1** has been included as the reference compound. Results obtained with previously described compounds **9b** and **9a** (R₁ = 2- and 3-methylphenyl, respectively) have been included for comparison with newly synthesized compounds. Parent compounds **2–4**, bearing a 4-methylphenyl moiety as R₁, have also been included into Table 1.

In the 2-methylphenyl series (compounds **9b–e**), the R₂ *n*-butyl chain of analogue **9d** was found to be the best substituent and produced a 3- to 10-fold increase in activity compared to other compounds of the series (**9c** with an isopropyl chain as R₂ being the less active). Regarding the difference of activity between the two isoforms, all compounds were characterized by an isoform selectivity ratio (IC₅₀ TPα/IC₅₀ TPβ) of ~16–17 in this 2-substituted series except for analogue **9b** with R₂ = *n*-pentyl which had a lower ratio of 9. The higher ratio clearly suggested increased selectivity for TPβ relative to TPα. Meta substitution of the phenyl ring R₁ (3-methylphenyl series) seemed to have little influence on activity, except for compound **9h** characterized by a ~2- (compared to **9d**) to 20-fold (compared to **9c**) increase in activity on both isoforms. More interestingly, the compound **9h** estimated selectivity ratio was the highest in this table (23.2, Table 1) whereas other compounds of this series displayed a ~10 fold ratio. In previous work, the compounds having a 4-methylphenyl moiety as the aromatic ring R₁ proved generally to be the most potent on TPα.¹³ The two original R₂ alkyl chains evaluated in this aryloxy series, *n*-propyl (**9j**) and isopropyl (**9i**), produced an important (~10 fold) decrease of activity on both isoforms. Collectively, the results of Table 1 highlighted the following general trend for most active R₂ substituents on both isoforms: *tert*-butyl ≈

Table 1. Estimated IC₅₀ Values for the Inhibition of [Ca²⁺]_i Mobilization Mediated by Either TPα or TPβ upon Stimulation by U46619 (1 μM). First Series: Influence of the Position of R₁ Methyl Substituent and of the Side Chain

compd	R ₁	R ₂	Y	inhibition of U46619-mediated [Ca ²⁺] _i mobilization (IC ₅₀ , nM) ^a		ratio ^b
				TPα	TPβ	
1	4-methylphenyl	<i>tert</i> -butyl	NH	319 ± 203	53 ± 19	6.01
2^c	4-methylphenyl	<i>tert</i> -butyl	O	58 ± 43	58 ± 4	1.0
3^c	4-methylphenyl	<i>n</i> -pentyl	O	139 ± 88	55 ± 5	2.5
4^c	4-methylphenyl	<i>n</i> -butyl	O	558 ± 34	53 ± 2	10.5
9a	3-methylphenyl	<i>n</i> -pentyl	O	2530 ± 419	223 ± 68	11.3
9b	2-methylphenyl	<i>n</i> -pentyl	O	1630 ± 924	181 ± 101	9.0
9c	2-methylphenyl	isopropyl	O	8750 ± 446	501 ± 63	17.5
9d	2-methylphenyl	<i>n</i> -butyl	O	673 ± 339	42 ± 20	16.1
9e	2-methylphenyl	<i>tert</i> -butyl	O	3760 ± 637	233 ± 88	16.1
9f	3-methylphenyl	isopropyl	O	2640 ± 492	205 ± 132	12.9
9g	3-methylphenyl	<i>n</i> -butyl	O	1910 ± 689	155 ± 30	12.3
9h	3-methylphenyl	<i>tert</i> -butyl	O	398 ± 145	17 ± 8	23.2
9i	4-methylphenyl	isopropyl	O	8760 ± 3780	843 ± 124	10.4
9j	4-methylphenyl	<i>n</i> -propyl	O	4220 ± 2060	448 ± 328	9.4

^a Results are expressed as mean ± SD of three separate experiments. ^b IC₅₀TPα/IC₅₀TPβ. ^c Data already published.¹³

Table 2. Estimated IC₅₀ Values for the Inhibition of [Ca²⁺]_i Mobilization Mediated by Either TPα or TPβ upon Stimulation by U46619 (1 μM). Second Series: Influence of Nature and Position of R₁ Phenyl Ring Substituents

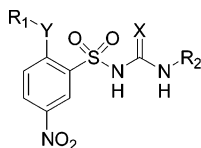
compd	R ₁	R ₂	Y	inhibition of U46619-mediated [Ca ²⁺] _i mobilization (IC ₅₀ , nM) ^a		ratio ^b
				TPα	TPβ	
1	4-methylphenyl	<i>tert</i> -butyl	NH	319 ± 203	53 ± 19	6.01
9k	2-bromophenyl	<i>tert</i> -butyl	O	2580 ± 1120	151 ± 73	17.0
9l	2-bromophenyl	<i>n</i> -pentyl	O	3130 ± 827	423 ± 164	7.4
9m	3-bromophenyl	<i>tert</i> -butyl	O	683 ± 189	59 ± 30	11.6
9n	3-bromophenyl	<i>n</i> -pentyl	O	5860 ± 2420	413 ± 303	14.2
9o	4-bromophenyl	<i>tert</i> -butyl	O	1660 ± 1290	523 ± 145	3.2
9p	4-bromophenyl	<i>n</i> -pentyl	O	1010 ± 257	120 ± 63	8.4
9q	2-chlorophenyl	<i>tert</i> -butyl	O	2420 ± 1780	205 ± 156	11.8
9r	2-chlorophenyl	<i>n</i> -pentyl	O	3060 ± 775	387 ± 178	7.9
9s	3-chlorophenyl	<i>tert</i> -butyl	O	698 ± 226	73 ± 9	9.6
9t	3-chlorophenyl	<i>n</i> -pentyl	O	2390 ± 526	201 ± 42	11.9
9u	4-chlorophenyl	<i>tert</i> -butyl	O	3050 ± 1670	400 ± 277	7.6
9v	4-chlorophenyl	<i>n</i> -pentyl	O	871 ± 362	98 ± 45	8.9
9w	3-iodophenyl	<i>tert</i> -butyl	O	470 ± 153	95 ± 35	4.9
9x	3-iodophenyl	<i>n</i> -pentyl	O	4520 ± 1800	885 ± 389	5.1
9y	4-iodophenyl	<i>tert</i> -butyl	O	2150 ± 307	401 ± 212	5.4
9z	4-iodophenyl	<i>n</i> -pentyl	O	2190 ± 1180	302 ± 153	7.2

^a Results are expressed as mean ± SD of three separate experiments. ^b IC₅₀TPα/IC₅₀TPβ.

n-butyl > *n*-pentyl ≥ *n*-propyl ≅ isopropyl. For compounds with *tert*-butyl and *n*-pentyl chains, the best substitution positions for activity on both isoforms were 4 > 3 ≥ 2. Regarding the selectivity, the best alkyl side chain was R₂ = *n*-butyl or *tert*-butyl, and the following trend was observed for these side chains regarding the phenyl ring substitution: 3 ≥ 2 ≫ 4.

Furthermore, we designed compounds to address the specific role in selectivity and activity of the nature of the substituent on the phenyl ring R₁. Former results showed that, in other series, combination of a methyl or bromo substituent in the 4-position of the second ring with a *n*-pentyl side chain favored the TPβ activity while some compounds with no substituents in these positions showed a high affinity and activity on TPα.¹³

Consequently, we wished to compare the methyl group with several other substituents. To this end, we designed and prepared compounds which were characterized by a halogen atom instead of the methyl group. Thus, monosubstituted derivatives with a chlorine, bromine, and iodine atom in the 2-(except for iodine series), 3-, and 4-position were synthesized (**9k–z**, Scheme 2). For each compound, two alkyl side chains R₂ were envisaged: *tert*-butyl and *n*-pentyl, in order to collect information on the influence of a long linear or short globular chain in this series. Table 2 shows that the replacement of a methyl group by a bromine atom had little or no positive effect, both in terms of potency and selectivity. It is interesting to note that compound **9m** (3-bromophenyl) had a ~2 fold decrease of selectivity ratio

Table 3. Estimated IC₅₀ Values for the Inhibition of [Ca²⁺]_i Mobilization Mediated by Either TPα or TPβ upon Stimulation by U46619 (1 μM). Third Series: Influence of Large Substituent at Position 4 of R₁ Aromatic Ring and Polysubstitution of R₁

compd	R ₁	R ₂	Y	inhibition of U46619-mediated [Ca ²⁺] _i mobilization (IC ₅₀ , nM) ^a		ratio ^b
				TPα	TPβ	
1	4-methylphenyl	<i>tert</i> -butyl	NH	319 ± 203	53 ± 19	6.01
9aa	4-methoxyphenyl	<i>tert</i> -butyl	O	1940 ± 343	152 ± 76	12.7
9ab	4-methoxyphenyl	<i>n</i> -pentyl	O	2670 ± 1970	446 ± 416	6.0
9ac	4-propoxyphenyl	<i>tert</i> -butyl	O	10760 ± 5150	875 ± 238	12.3
9ad	4-propoxyphenyl	<i>n</i> -pentyl	O	27230 ± 2650	4840 ± 2520	5.6
9ae	4-ethoxyphenyl	<i>tert</i> -butyl	O	19190 ± 11410	1100 ± 401	17.5
9af	4-ethoxyphenyl	<i>n</i> -pentyl	O	13560 ± 3440	749 ± 59	18.1
9ag	3-methoxyphenyl	<i>tert</i> -butyl	O	1970 ± 622	99 ± 61	19.9
9ah	3-methyl-4-chlorophenyl	<i>tert</i> -butyl	O	1060 ± 207	111 ± 54	9.6
9ai	3-methyl-4-chlorophenyl	<i>n</i> -pentyl	O	3720 ± 769	565 ± 200	6.6
9aj	2-methoxy-4-methylphenyl	<i>tert</i> -butyl	O	528 ± 133	52 ± 10	10.2

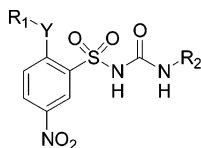
^a Results are expressed as mean ± SD of three separate experiments. ^b IC₅₀TPα/IC₅₀TPβ.

compared with its potent methylated analogue **9h** (11.6 and 23.2, respectively). Consistent with our previous observation on the activity trend, **9m**, with a substituent in the 3-position and a *tert*-butyl R₂ alkyl chain, was the most potent compound of its series. Compounds of the 4-bromophenyl series were less potent than their methyl counterparts, but kept the same rank order of selectivity ratio. In the chlorophenyl series, the same trends were observed, with little differences compared to the bromophenyl compounds series. Once again, the 3-position substitution of phenyl ring combined with a *tert*-butyl side chain produced the most potent compound, **9s**, both on TPα and TPβ (Table 2). Interestingly, in the iodophenyl series, although compound potencies were in the same range as the other halo-substituted compounds, the selectivity ratio was diminished. To this extent, compound **9w** was the most representative since its 3-position substitution along with a *tert*-butyl side chain R₂ increased its TPα potency while decreasing its TPβ activity (Table 2). Thus, **9w** was the most potent TPα halo-substituted antagonist in this table with a potency close to that of **9h** (TPα IC₅₀ 470 ± 153 nM and 398 ± 145 nM, respectively). From this table (Table 2), we can presume that the best combination for our derivatives is a substituent at the 3-position of the phenyl ring R₁ and a *tert*-butyl side chain R₂. The following trends have been observed within these series: TPα activity: CH₃ ≅ I > Cl ≅ Br; TPβ activity: CH₃ > Br ≅ Cl > I; selectivity toward TPβ isoform: CH₃ > Br ≅ Cl > I. Additionally, it is interesting to point out that within bromo and chloro derivatives, the combination of a 4-substituted phenyl moiety with a *n*-pentyl side chain produced the most selective compounds whereas, surprisingly, in the 4-iodo series, compounds were less selective. In the series with a 3-substituted phenyl moiety (bromo, chloro, and iodo), a *tert*-butyl side chain produced a ~10 fold increase in activity compared to compounds with *n*-pentyl side chain (Table 2).

We subsequently aimed to explore the influence of longer substituents at the 4-position of the second aromatic ring R₁. Consequently, several derivatives with a 4-alkoxyphenyl moiety as R₁ were prepared (**9aa–af**, Scheme 2). Moreover, some disubstituted compounds were synthesized (**9ag–aj**). The R₂ alkyl chain in this series was either a *tert*-butyl or a *n*-pentyl moiety. We observed a systematically important loss of activity on both isoforms for compounds with alkoxy groups at the

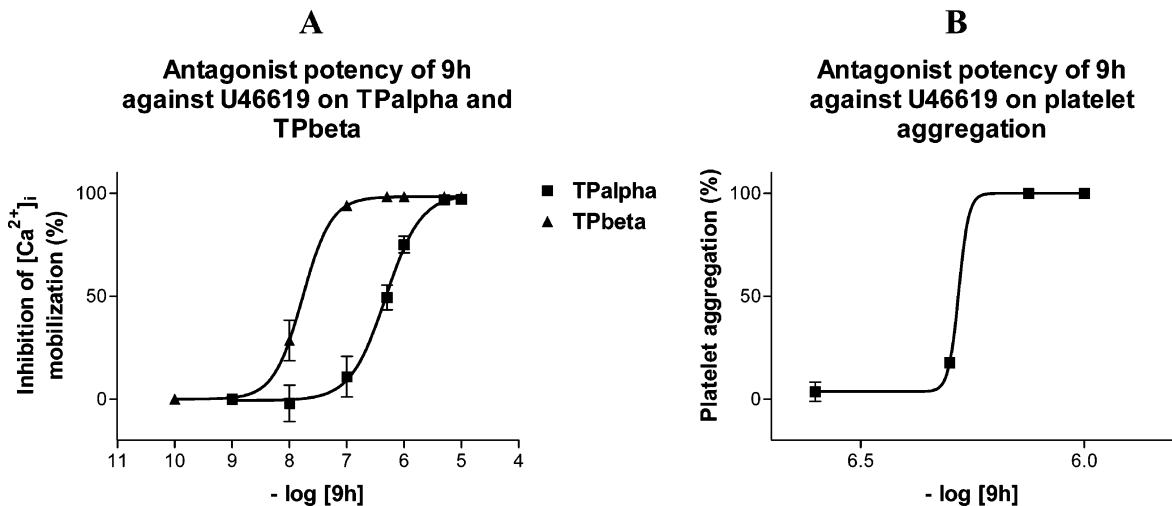
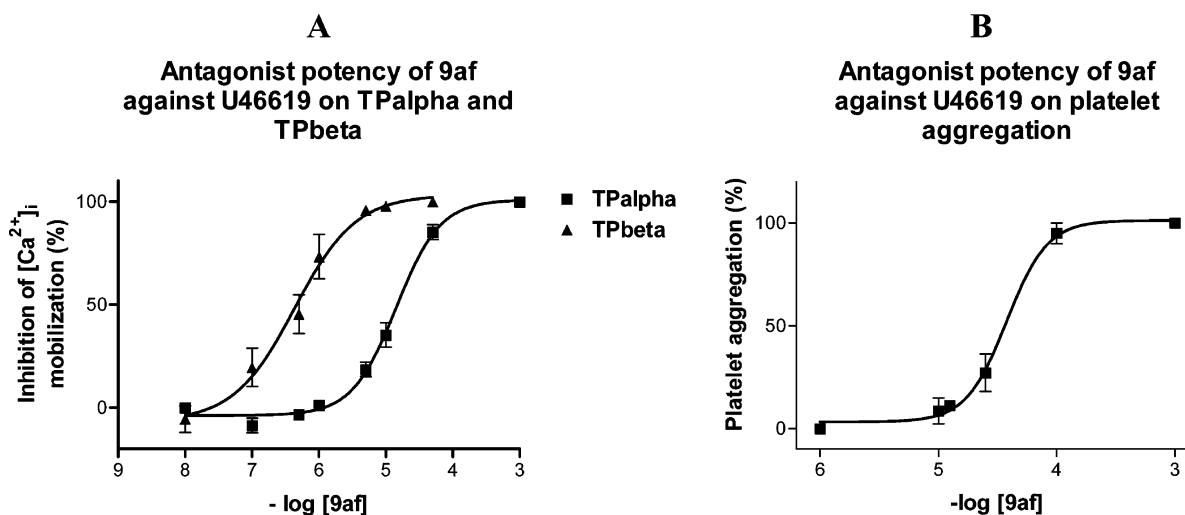
4-position of the phenyl ring R₁ compared with the parent methylated compounds (**2** and **3**). For both side chains (R₂ = *tert*-butyl or *n*-pentyl), the loss of activity depended on the length of the alkoxy group. Interestingly, the activity on TPβ decreased less markedly than activity on TPα, thus increasing the selectivity ratio toward the TPβ isoform (4-ethoxyphenyl, **9ae** and **9af** > 4-methoxyphenyl, **9aa** ≅ 4-propoxyphenyl, **9ac**). The most interesting compound of this table (**9ag**) was obtained with the combination of a methoxy group in the 3-position of the phenyl ring R₁ and the R₂ side chain being a *tert*-butyl moiety. Fully consistent with observations in other series, this compound displayed a potent antagonism of TPβ-mediated [Ca²⁺]_i mobilization combined with a good selectivity ratio (19.9). The particular interest of this compound is that, although slightly less potent than its methylated or halogenated analogues (**9h**, **9m**, **9s**, or **9w**) on TPβ (IC₅₀ = ~99 nM), it is characterized by a much lower activity on TPα (IC₅₀ = ~2 μM). Disubstituted compounds **9ah** and **9ai** proved to have a combined profile of monosubstituted 4-chlorophenyl and 3-methylphenyl analogues (**9u**, **v** and **9a–h**, respectively). Thus, the presence of a methyl group at the 3-position of compound **9u** increased ~3–4 fold its activity, without reaching the potent activity of the solely 3-methyl-substituted **9h** (Tables 3 and 1, respectively). The presence of a 2-methoxy group concomitant with a 4-methyl group on the phenyl ring had little influence on TPβ activity but decreased ~10 fold the TPα activity compared to **2** (Tables 3 and 1, respectively). Since cyanoguanidines proved to be quite active at both isoforms in other series,¹³ we synthesized an oxygen-bonded cyanoguanidine, **10** (Scheme 3). This replacement of sulfonylurea had a negative impact on the activity and generated an inferior selectivity ratio (Table 4).

Finally, within this “oxygen-bridged” family of chemical compounds, we wished to confirm the antiplatelet activity of the most potent compounds. Selection relied on their activity on TPα and TPβ or the importance of their selectivity ratio. **9h** was the first to be evaluated because it displayed the optimal structure for both activity and selectivity among the compounds presented herein. The IC₅₀ of compound **9h** for inhibition of U46619-induced platelet aggregation was found to be similar to the one for the inhibition of [Ca²⁺]_i mobilization triggered by TPα isoform (513 ± 28 nM and 398 ± 145 nM, respectively). The concentration–response curve obtained with this

Table 4. Estimated IC₅₀ Values for the Inhibition of [Ca²⁺]_i Mobilization Mediated by Either TPα or TPβ upon Stimulation by U46619 (1 μM). Fourth Series: Impact of the Sulfonylurea Function

compd	R ₁	R ₂	Y	X	inhibition of U46619-mediated [Ca ²⁺] _i mobilization (IC ₅₀ , nM) ^a		ratio ^b
					TPα	TPβ	
1	4-methylphenyl	<i>tert</i> -butyl	NH	O	319 ± 203	53 ± 19	6.01
13c	4-methylphenyl	<i>tert</i> -butyl	O	N-C N	2080 ± 179	579 ± 53	3.6

^a Results are expressed as mean ± SD of three separate experiments. ^b IC₅₀TPα/IC₅₀TPβ.

**Figure 2.** (A) Concentration–response curves for inhibition of [Ca²⁺]_i mobilization by 9 h on separate isoforms. (B) Concentration response curve for inhibition of platelet aggregation by 9 h.**Figure 3.** (A) Concentration–response curves for inhibition of [Ca²⁺]_i mobilization by 9af on separate isoforms. (B) Concentration response curve for inhibition of platelet aggregation by 9af.

compound on platelets can overlay the TPα curve (Figure 2, panels A and B). These results confirmed the theory postulating that platelet aggregation is solely mediated by TPα isoform. It is noteworthy that **9h** is inactive or almost inactive on TPα (expressed in platelets and in HEK·TPα cells) when tested at 0.1 μM, although it has complete antagonistic activity on TPβ (expressed in HEK·TPβ cells) at this concentration (Figure 2, panel A). Thus, this compound is theoretically selective for TPβ at this concentration.

We have conducted similar experiments on platelets with other potentially selective compounds. Thus, **9af** displayed a similar profile with comparable IC₅₀s for inhibition of U46619-induced platelet aggregation and [Ca²⁺]_i mobilization. This compound had nevertheless its curves strongly shifted to the right in inhibition of [Ca²⁺]_i mobilization (Figure 3, panel A) and was thus less active on platelets (IC₅₀: 40 ± 9 μM, Figure 3, panel B). Consequently, with a selectivity ratio within the same rank order, it could be more interesting since it is almost

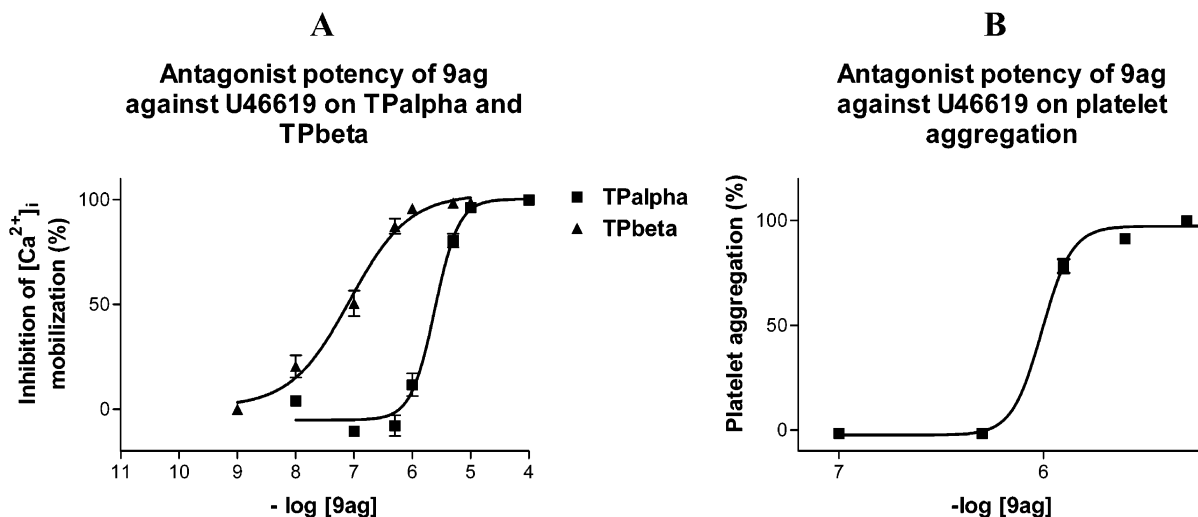


Figure 4. (A) Concentration–response curves for inhibition of $[Ca^{2+}]_i$ mobilization by **9ag** on separate isoforms. (B) Concentration response curve for inhibition of platelet aggregation by **9ag**.

inactive on platelets at concentrations below 10 μ M but keeps a good activity on TP β isoform expressed in HEK293 cell lines. Similarly, compound **9ag** was one of the most interesting compounds, since it displayed one of the best activity on TP β , while being poorly active on platelets (IC_{50} : 985 ± 49 nM) (Figure 4).

Conclusions

TXA₂ exerts its proaggregatory and constrictive actions upon binding to specific GPCR named TP. In humans, two isoforms (TP α and TP β) of this receptor have been described that differ exclusively in their C-carboxyl terminal tail domains. Herein, we present the design, synthesis and SAR study of a series of 35 original *N*-alkyl-*N'*-[2-(aryloxy)-5-nitrobenzenesulfonyl]ureas and -cyanoguanidines. These compounds were designed based on a previous report by our group that highlighted this family as potentially interesting in terms of antagonistic activity as well as selectivity toward the individual TP isoforms. Results obtained in an inhibition of $[Ca^{2+}]_i$ mobilization test performed on both TP α and TP β isoforms allowed us to define the optimal nature and position of several structural moieties for both activity and selectivity. The study represents the first extended SAR study dealing with selectivity among TP receptor isoforms. Three compounds were selected for their selectivity and activity, and their TP α antagonistic potency was confirmed in a human platelet aggregation test.

Experimental Section

Chemistry. All commercial chemicals (Sigma-Aldrich, Belgium) and solvents are reagent grade and were used without further purification unless otherwise stated. Compounds **1**, **7**,¹⁶ **2**, **3**, **4**, **8a,b**, and **9a,b**¹³ were synthesized as previously described. 2-(2-Methylphenoxy)-5-nitrobenzenesulfonamide (**8c**) was commercially available (AmbinterStock Screening Collection). Nevertheless, this compound was synthesized in our lab according to the method of preparation described below. All reactions were followed by thin-layer chromatography (Silicagel 60F₂₅₄ Merck), and visualization was accomplished with UV light (254 nm). Elemental analyses (C, H, N, S) were determined on a Carbo Erba EA 1108 and were within $\pm 0.4\%$ of the theoretical values. NMR spectra were recorded on a Bruker Avance 500 spectrometer using DMSO-*d*₆ or CDCl₃ as solvent and tetramethylsilane as internal standard. For ¹H NMR spectra, chemical shifts are expressed in δ (ppm) downfield from tetramethylsilane. The abbreviations s, singlet; d, doublet; t,

triplet; m, multiplet; br, broad were used throughout. Infrared spectra were recorded using a Perkin-Elmer FT-IR 1750. All compounds described were recrystallized from hot methanol (40 °C)/H₂O mixture (60/40; 10 mL/100 mg of product) unless otherwise stated.

General Procedure for the Reaction of 7 with Phenols. Before the reaction was started, the phenolates were obtained from the corresponding cresols (0.05 mol) after their neutralization by 0.06 M NaOH (in aqueous solution, 10% w/v) in acetone. Evaporation under reduced pressure provided crystals of the phenolates.

Compound **7** (0.01 mol) and the appropriate phenolate (0.05 mol) were dissolved in acetonitrile. The mixture was refluxed, and potassium carbonate (0.007 mol) was added. After completion of the reaction monitored by TLC (12–36 h), the solution was acidified by means of hydrochloric acid solution (10 M) and filtered, and the filtrate was evaporated under reduced pressure. The crude product was dissolved in methanol, and ice was added. The resulting precipitate was collected by filtration. (Yield: 60–70%).

2-(4-Chlorophenoxy)-5-nitrobenzenesulfonamide (8d). Mp: 180–181 °C. Anal. (C₁₂H₉ClN₂O₅S) C, H, N, S.

2-(3-Chlorophenoxy)-5-nitrobenzenesulfonamide (8e). Mp: 128–130 °C. Anal. (C₁₂H₉ClN₂O₅S) C, H, N, S.

2-(2-Chlorophenoxy)-5-nitrobenzenesulfonamide (8f). Mp: 170–171 °C. Anal. (C₁₂H₉ClN₂O₅S) C, H, N, S.

2-(4-Bromophenoxy)-5-nitrobenzenesulfonamide (8g). Mp: 170–171 °C. Anal. (C₁₂H₉BrN₂O₅S) C, H, N, S.

2-(3-Bromophenoxy)-5-nitrobenzenesulfonamide (8h). Mp: 149–150 °C. Anal. (C₁₂H₉BrN₂O₅S) C, H, N, S.

2-(2-Bromophenoxy)-5-nitrobenzenesulfonamide (8i). Mp: 190–192 °C. Anal. (C₁₂H₉BrN₂O₅S) C, H, N, S.

2-(4-Iodophenoxy)-5-nitrobenzenesulfonamide (8j). Mp: 178–179 °C. Anal. (C₁₂H₉I₂O₅S) C, H, N, S.

2-(3-Iodophenoxy)-5-nitrobenzenesulfonamide (8k). Mp: 153–154 °C. Anal. (C₁₂H₉I₂O₅S) C, H, N, S.

2-(4-Methoxyphenoxy)-5-nitrobenzenesulfonamide (8l). Mp: 161–166 °C. Anal. (C₁₃H₁₂N₂O₆S) C, H, N, S.

2-(4-Propoxyphenoxy)-5-nitrobenzenesulfonamide (8m). Mp: 135–138 °C. Anal. (C₁₅H₁₆N₂O₆S) C, H, N, S.

2-(4-Ethoxyphenoxy)-5-nitrobenzenesulfonamide (8n). Mp: 158–162 °C. Anal. (C₁₄H₁₄N₂O₆S) C, H, N, S.

2-(3-Methyl-4-chlorophenoxy)-5-nitrobenzenesulfonamide (8o). Mp: 182–184 °C. Anal. (C₁₃H₁₁ClN₂O₅S) C, H, N, S.

2-(3-Methoxyphenoxy)-5-nitrobenzenesulfonamide (8p). Mp: 136–137 °C. Anal. (C₁₃H₁₂N₂O₆S) C, H, N, S.

General Procedure for the Preparation of Sulfonylureas with Isocyanates. The appropriate sulfonamide (0.01 mol) was dissolved in acetone (30 mL), and 0.01 mol NaOH (10% aqueous sol. w/v) was added. The mixture was gently mixed during 10 min and then

was evaporated under reduced pressure. The resulting solid was resuspended in acetone (30 mL) and gently refluxed. The appropriate isocyanate (0.02 mol) was added to the mixture. At the end of the reaction (0.1–1 h), the mixture was evaporated under reduced pressure, and the crude product was washed with AcOEt. The solid was collected by filtration and dissolved in an aqueous NaOH solution (0.5 N; 20 mL). The resulting solution was adjusted to pH = 1 with hydrochloric acid (12 N), and the solid which precipitated was isolated by filtration (Yield: 40–60%).

***N*-Isopropyl-*N'*-[2-(2-methylphenoxy)-5-nitrobenzenesulfonyl]urea (9c).** Mp: 196–198 °C. Anal. (C₁₉H₁₉N₃O₆S) C, H, N, S.

***N*-*n*-Butyl-*N'*-[2-(2-methylphenoxy)-5-nitrobenzenesulfonyl]urea (9d).** Mp: 179–181 °C. Anal. (C₁₈H₂₁N₃O₆S) C, H, N, S.

***N*-*tert*-Butyl-*N'*-[2-(2-methylphenoxy)-5-nitrobenzenesulfonyl]urea (9e).** Mp: 150–153 °C. Anal. (C₁₈H₂₁N₃O₆S) C, H, N, S.

***N*-Isopropyl-*N'*-[2-(3-methylphenoxy)-5-nitrobenzenesulfonyl]urea (9f).** Mp: 173–174 °C. Anal. (C₁₇H₁₉N₃O₆S) C, H, N, S.

***N*-*n*-Butyl-*N'*-[2-(3-methylphenoxy)-5-nitrobenzenesulfonyl]urea (9g).** Mp: 183–184 °C. Anal. (C₁₈H₂₁N₃O₆S) C, H, N, S.

***N*-*tert*-Butyl-*N'*-[2-(3-methylphenoxy)-5-nitrobenzenesulfonyl]urea (9h).** Mp: 150–152 °C. Anal. (C₁₈H₂₁N₃O₆S) C, H, N, S.

***N*-Isopropyl-*N'*-[2-(4-methylphenoxy)-5-nitrobenzenesulfonyl]urea (9i).** Mp: 183–184 °C. Anal. (C₁₇H₁₉N₃O₆S) C, H, N, S.

***N*-*n*-Propyl-*N'*-[2-(4-methylphenoxy)-5-nitrobenzenesulfonyl]urea (9j).** Mp: 206–208 °C. Anal. (C₁₇H₁₉N₃O₆S) C, H, N, S.

***N*-*tert*-Butyl-*N'*-[2-(2-bromophenoxy)-5-nitrobenzenesulfonyl]urea (9k).** Mp: 169–173 °C. Anal. (C₁₇H₁₈BrN₃O₆S) C, H, N, S.

***N*-*n*-Pentyl-*N'*-[2-(2-bromophenoxy)-5-nitrobenzenesulfonyl]urea (9l).** Mp: 130–135 °C. Anal. (C₁₈H₂₀BrN₃O₆S) C, H, N, S.

***N*-*tert*-Butyl-*N'*-[2-(3-bromophenoxy)-5-nitrobenzenesulfonyl]urea (9m).** Mp: 148–149 °C. Anal. (C₁₇H₁₈BrN₃O₆S) C, H, N, S.

***N*-*n*-Pentyl-*N'*-[2-(3-bromophenoxy)-5-nitrobenzenesulfonyl]urea (9n).** Mp: 136–138 °C. Anal. (C₁₈H₂₀BrN₃O₆S) C, H, N, S.

***N*-*tert*-Butyl-*N'*-[2-(4-bromophenoxy)-5-nitrobenzenesulfonyl]urea (9o).** Mp: 173–174 °C. Anal. (C₁₇H₁₈BrN₃O₆S) C, H, N, S.

***N*-*n*-Pentyl-*N'*-[2-(4-bromophenoxy)-5-nitrobenzenesulfonyl]urea (9p).** Mp: 166–168 °C. Anal. (C₁₈H₂₀BrN₃O₆S) C, H, N, S.

***N*-*tert*-Butyl-*N'*-[2-(2-chlorophenoxy)-5-nitrobenzenesulfonyl]urea (9q).** Mp: 186–187 °C. Anal. (C₁₇H₁₈ClN₃O₆S) C, H, N, S.

***N*-*n*-Pentyl-*N'*-[2-(2-chlorophenoxy)-5-nitrobenzenesulfonyl]urea (9r).** Mp: 132–133 °C. Anal. (C₁₈H₂₀ClN₃O₆S) C, H, N, S.

***N*-*tert*-Butyl-*N'*-[2-(3-chlorophenoxy)-5-nitrobenzenesulfonyl]urea (9s).** Mp: 154–156 °C. Anal. (C₁₇H₁₈ClN₃O₆S) C, H, N, S.

***N*-*n*-Pentyl-*N'*-[2-(3-chlorophenoxy)-5-nitrobenzenesulfonyl]urea (9t).** Mp: 158–159 °C. Anal. (C₁₈H₂₀ClN₃O₆S) C, H, N, S.

***N*-*tert*-Butyl-*N'*-[2-(4-chlorophenoxy)-5-nitrobenzenesulfonyl]urea (9u).** Mp: 161–163 °C. Anal. (C₁₇H₁₈ClN₃O₆S) C, H, N, S.

***N*-*n*-Pentyl-*N'*-[2-(4-chloroxyphenoxy)-5-nitrobenzenesulfonyl]urea (9v).** Mp: 162–164 °C. Anal. (C₁₈H₂₀ClN₃O₆S) C, H, N, S.

***N*-*tert*-Butyl-*N'*-[2-(3-iodophenoxy)-5-nitrobenzenesulfonyl]urea (9w).** Mp: 154–157 °C. Anal. (C₁₇H₁₈IN₃O₆S) C, H, N, S.

***N*-*n*-Pentyl-*N'*-[2-(3-iodophenoxy)-5-nitrobenzenesulfonyl]urea (9x).** Mp: 123–126 °C. Anal. (C₁₈H₂₀IN₃O₆S) C, H, N, S.

***N*-*tert*-Butyl-*N'*-[2-(4-iodophenoxy)-5-nitrobenzenesulfonyl]urea (9y).** Mp: 176–179 °C. Anal. (C₁₇H₁₈IN₃O₆S) C, H, N, S.

***N*-*n*-Pentyl-*N'*-[2-(4-iodophenoxy)-5-nitrobenzenesulfonyl]urea (9z).** Mp: 151–154 °C. Anal. (C₁₈H₂₀IN₃O₆S) C, H, N, S.

***N*-*tert*-Butyl-*N'*-[2-(4-methoxyphenoxy)-5-nitrobenzenesulfonyl]urea (9aa).** Mp: 176–177 °C. Anal. (C₁₈H₂₁N₃O₇S) C, H, N, S.

***N*-*n*-Pentyl-*N'*-[2-(4-methoxyphenoxy)-5-nitrobenzenesulfonyl]urea (9ab).** Mp: 170–172 °C. Anal. (C₁₉H₂₃N₃O₇S) C, H, N, S.

***N*-*tert*-Butyl-*N'*-[2-(4-propoxyphenoxy)-5-nitrobenzenesulfonyl]urea (9ac).** Mp: 145–149 °C. Anal. (C₂₀H₂₅N₃O₇S) C, H, N, S.

***N*-*n*-Pentyl-*N'*-[2-(4-propoxyphenoxy)-5-nitrobenzenesulfonyl]urea (9ad).** Mp: 148–150 °C. Anal. (C₂₁H₂₇N₃O₇S) C, H, N, S.

***N*-*tert*-Butyl-*N'*-[2-(4-ethoxyphenoxy)-5-nitrobenzenesulfonyl]urea (9ae).** Mp: 178–179 °C. Anal. (C₁₉H₂₃N₃O₇S) C, H, N, S.

***N*-*n*-Pentyl-*N'*-[2-(4-ethoxyphenoxy)-5-nitrobenzenesulfonyl]urea (9af).** Mp: 182–185 °C. Anal. (C₂₀H₂₅N₃O₇S) C, H, N, S.

***N*-*tert*-Butyl-*N'*-[2-(3-methoxyphenoxy)-5-nitrobenzenesulfonyl]urea (9ag).** Mp: 128–131 °C. Anal. (C₁₈H₂₁N₃O₇S) C, H, N, S.

***N*-*tert*-Butyl-*N'*-[2-(3-methyl-4-chlorophenoxy)-5-nitrobenzenesulfonyl]urea (9ah).** Mp: 174–176 °C. Anal. (C₁₈H₂₀ClN₃O₆S) C, H, N, S.

***N*-*n*-Pentyl-*N'*-[2-(3-methyl-4-chlorophenoxy)-5-nitrobenzenesulfonyl]urea (9ai).** Mp: 174–176 °C. Anal. (C₁₉H₂₂ClN₃O₆S) C, H, N, S.

***N*-*tert*-Butyl-*N'*-[2-(2-methoxy-4-methylphenoxy)-5-nitrobenzenesulfonyl]urea (9aj).** Mp: 160–162 °C. Anal. (C₁₉H₂₃N₃O₇S) C, H, N, S.

Procedure for the Preparation of *N*-*tert*-Butyl-*N'*-cyano-*O*-phenylisourea (11). A mixture of **10** (0.01 mol) and *tert*-butylamine (0.015 mol) in 2-propanol (30 mL) was stirred at room temperature for 10–15 min. The solution was evaporated, and the crude oil was crystallized in cold methanol. Mp: 134–136 °C. ¹H NMR (DMSO) δ: 0.86 (t, 2H, *J* = 9 Hz, NHCH₂CH₂CH₂CH₂CH₃); 1.1–1.35 (m, 6H, NHCH₂CH₂CH₂CH₂CH₃); 3.26 (q, 2H, *J* = 9 Hz, NHCH₂CH₂CH₂CH₂CH₃); 7.06–7.41 (m, 5H, H_{ar}o).

Procedure for the Preparation of *N*-*tert*-Butyl-*N'*-[2-(4-methylphenoxy)-5-nitrobenzenesulfonyl]-*N'*-cyanoguanidine (12). The appropriate sulfonamide (0.01 mol) was dissolved in acetone (30 mL). NaOH (0.01 mol, 10% aqueous sol. w/v) was added. The mixture was gently mixed during 10 min and was evaporated under reduced pressure. The solid was resuspended in dimethylformamide (20 mL) at room temperature, and the appropriate *N*-alkyl-*N'*-cyano-*O*-phenylisourea was added. The mixture was stirred at RT for 20–24 h. At the end of the reaction, the mixture was evaporated under reduced pressure and the crude oil was suspended in a mixture of methanol and hydrochloric acid (5 N aqueous solution) from which crystals of the desired product appeared. Mp: 161–163 °C. Anal. (C₁₉H₂₁N₅O₅S) C, H, N, S.

Calcium Measurements. HEK·TP α and HEK·TP β cell lines, stably overexpressing HA-tagged forms of TP α and TP β in human embryonic kidney (HEK) 293 cells have been previously described.⁸ HEK 293 cells or their stable cell line equivalents were routinely grown in Dulbecco's modified Eagle's medium (DMEM) containing 10% fetal bovine serum (FBS). Measurement of [Ca²⁺]_i mobilization either in HEK·TP α or HEK·TP β cells was carried out using fluorescent microplate reader Fluoroskan Ascent FL equipped with two dispenser (Thermo Electron Corporation, Finland) according to modified method of Lin et al.¹⁷ Briefly, cells were trypsinized and washed twice with Krebs-HEPES buffer (118 mM, NaCl, 4.7 mM KCl, 1.2 mM MgSO₄, 1.2 mM KH₂PO₄, 4.2 mM NaHCO₃, 11.7 mM D-glucose, 1.3 mM CaCl₂, 10 mM HEPES, pH 7.4) and incubated for 1 h with fluorescent dye Fluo-4/AM (5 μg/mL; Molecular Probes, Invitrogen, Merelbeke, Belgium). Cells were then rinsed three times with Krebs-HEPES buffer, and 150 μL of a suspension of cells in that buffer was loaded into each well of a 96-well plate at a density of 150 000 cells/well. Cells were incubated 10 min with various concentrations of the test compound (10⁻⁵ to 10⁻⁸ M final; 10 μL) prior to stimulation with U46619 (1 μM final, 50 μL). In all cases, compound (1 mM) was diluted in dimethyl sulfoxide (DMSO)/PBS (30/70) prior to further dilution in PBS. Fluorescence emission was read at 538 nm. At the end of each experiment, fluorescence intensities were calibrated for determination of intracellular calcium concentration ([Ca²⁺]_i) values by permeabilizing cells with 1% Triton X-100 to release all the dye (F_{max}) and subsequently chelating with 10 mM EGTA (F_{min}). Calcium concentrations were calculated using equation [Ca²⁺]_i = K_d(F - F_{min})/(F_{max} - F), assuming a K_d of 385 nM for Fluo-4. The results (IC₅₀) presented are the concentration required to inhibit 50% of the normal rise of [Ca²⁺]_i upon stimulation with 1 μM U46619, determined in the absence of any compounds. The IC₅₀ were calculated by nonlinear regression analysis (GraphPad Prism software) from at least three concentration–response curves.

Human In Vitro Platelet Aggregation. The antiaggregatory potency has been determined according to the turbidimetric Born's

method.¹⁸ The blood was drawn from 10 healthy donors of both genders, aged 20–30. The subjects were free from medication for at least 14 days. No significant differences in the results were observed between the donors in our experiments. Platelet-rich plasma (PRP) and platelet-poor plasma (PPP) were prepared as previously described.¹³ Platelet concentration of PRP was adjusted to 3×10^8 cells/mL by dilution with PPP. Platelet aggregation of PRP was studied using a double channel aggregometer (Chronolog Corporation, Chicago, IL). PRP (294 μ L) was added in a silanized cuvette and stirred (1000 rpm). Each drug was diluted (1 mM) in dimethyl sulfoxide (DMSO)/PBS (30/70) and preincubated in PRP for 3 min at 37 °C before the aggregating agent was added. Platelet aggregation was initiated by addition of a fresh solution of U46619 (1 μ M final). To evaluate platelet aggregation, the maximum increase in light transmission was determined from the aggregation curve 6 min after addition of the inducer. The drug concentration preventing 50% of platelet aggregation (IC_{50}) induced by arachidonic acid and U46619 was calculated by nonlinear regression analysis (GraphPad Prism software) from at least three dose–response curves.

Acknowledgment. Julien Hanson is funded by the “Fonds pour la Formation à la Recherche dans l’Industrie et dans l’Agriculture” (F.R.I.A., from Belgium). This work was supported by a grant from the “Fonds National de la Recherche Scientifique” (FNRS) from Belgium. The authors wish to thank M. Philippe Neven for excellent technical assistance. B.T. Kinsella acknowledges the financial support of the Wellcome Trust and Science Foundation Ireland.

Supporting Information Available: NMR, elemental analysis, melting points, and IR peaks for all compounds presented. This material is available free of charge via the Internet at <http://pubs.acs.org>.

References

- (1) Hamberg, M.; Svensson, J.; Samuelsson, B. Thromboxanes: a new group of biologically active compounds derived from prostaglandin endoperoxides. *Proc. Natl. Acad. Sci. U.S.A.* **1975**, *72*, 2994–2998.
- (2) Moncada, S.; Ferreira, S. H.; Vane, J. R. Bioassay of prostaglandins and biologically active substances derived from arachidonic acid. *Adv Prostaglandin Thromboxane Res.* **1978**, *5*, 211–236.
- (3) Dogne, J. M.; de Leval, X.; Hanson, J.; Frederich, M.; Lambermont, B., et al. New developments on thromboxane and prostacyclin modulators part I: thromboxane modulators. *Curr. Med. Chem.* **2004**, *11*, 1223–1241.
- (4) Coleman, R. A.; Smith, W. L.; Narumiya, S. International Union of Pharmacology classification of prostanoid receptors: properties, distribution, and structure of the receptors and their subtypes. *Pharmacol. Rev.* **1994**, *46*, 205–229.
- (5) Hirata, M.; Hayashi, Y.; Ushikubi, F.; Yokota, Y.; Kageyama, R., et al. Cloning and expression of cDNA for a human thromboxane A2 receptor. *Nature* **1991**, *349*, 617–620.
- (6) Raychowdhury, M. K.; Yukawa, M.; Collins, L. J.; McGrail, S. H.; Kent, K. C., et al. Alternative splicing produces a divergent cytoplasmic tail in the human endothelial thromboxane A2 receptor. *J. Biol. Chem.* **1994**, *269*, 19256–19261.
- (7) Reid, H. M.; Kinsella, B. T. The alpha, but not the beta, isoform of the human thromboxane A2 receptor is a target for nitric oxide-mediated desensitization. Independent modulation of Tp alpha signaling by nitric oxide and prostacyclin. *J. Biol. Chem.* **2003**, *278*, 51190–51202.
- (8) Walsh, M. T.; Foley, J. F.; Kinsella, B. T. The alpha, but not the beta, isoform of the human thromboxane A2 receptor is a target for prostacyclin-mediated desensitization. *J. Biol. Chem.* **2000**, *275*, 20412–20423.
- (9) Kinsella, B. T. Thromboxane A2 signalling in humans: a ‘Tail’ of two receptors. *Biochem. Soc. Trans.* **2001**, *29*, 641–654.
- (10) Ashton, A. W.; Ware, J. A. Thromboxane A2 receptor signaling inhibits vascular endothelial growth factor-induced endothelial cell differentiation and migration. *Circ. Res.* **2004**, *95*, 372–379.
- (11) Habib, A.; FitzGerald, G. A.; Maclouf, J. Phosphorylation of the thromboxane receptor alpha, the predominant isoform expressed in human platelets. *J. Biol. Chem.* **1999**, *274*, 2645–2651.
- (12) Halushka, P. V. Thromboxane A(2) receptors: where have you gone? *Prostaglandins Other Lipid Mediat.* **2000**, *60*, 175–189.
- (13) Hanson, J.; Reynaud, D.; Qiao, N.; Devel, P.; Moray, A. L., et al. Synthesis and pharmacological evaluation of novel nitrobenzenic thromboxane modulators as antiplatelet agents acting on both the alpha and beta isoforms of the human thromboxane receptor. *J. Med. Chem.* **2006**, *49*, 3701–3709.
- (14) Dogne, J. M.; Hanson, J.; de Leval, X.; Kolh, P.; Tchana-Sato, V., et al. Pharmacological characterization of *N*-tert-butyl-*N'*-[2-(4'-methylphenylamino)-5-nitrobenzenesulfonyl]urea (BM-573), a novel thromboxane A2 receptor antagonist and thromboxane synthase inhibitor in a rat model of arterial thrombosis and its effects on bleeding time. *J. Pharmacol. Exp. Ther.* **2004**, *309*, 498–505.
- (15) Meerwein, H.; Dittmar, G.; Gollner, R.; Hafner, K.; Mensch, F., et al. Aromatic diazo compounds. II. Preparation of aromatic sulfonyl chlorides, a new modification of the Sandmeyer reaction. *Chem. Ber.* **1957**, *90*, 841–852.
- (16) Dogne, J. M.; Wouters, J.; Rolin, S.; Michaux, C.; Pochet, L., et al. Design, synthesis and biological evaluation of a sulfonylcyano-guanidine as thromboxane A2 receptor antagonist and thromboxane synthase inhibitor. *J. Pharm. Pharmacol.* **2001**, *53*, 669–680.
- (17) Lin, K.; Sadee, W.; Quillan, J. M. Rapid measurements of intracellular calcium using a fluorescence plate reader. *Biotechniques* **1999**, *26*, 318–322, 324–316.
- (18) Born, G. V.; Cross, M. J. The Aggregation of Blood Platelets. *J. Physiol.* **1963**, *168*, 178–195.

JM070427H